Applied Soft Computing Journal 81 (2019) 105486

Contents lists available at ScienceDirect

Applied Soft Computing Journal

journal homepage: www.elsevier.com/locate/asoc

Coordinated Traffic Light Control in Cooperative Green Vehicle Routing for Pheromone-based Multi-Agent Systems

Kian Lun Soon *, Joanne Mun-Yee Lim, Rajendran Parthiban

Electrical and Computer Systems Engineering, School of Engineering, Monash University, Jalan Lagoon Selatan, Bandar Sunway, 47500 Subang Jaya, Selangor, Malaysia

HIGHLIGHTS

- Green transportation was not well explored in existing pheromone framework.
- Pheromone-based Green Transportation System (PGTS) is proposed to reduce emissions.
- PGTS integrates coordinated traffic lights and cooperative green vehicle routing.
- This integration disperses upstream and downstream traffic to reduce fuel burnt.
- Vehicles can traverse intersections with fewer frequencies of acceleration in PGTS.

GRAPHICAL ABSTRACT

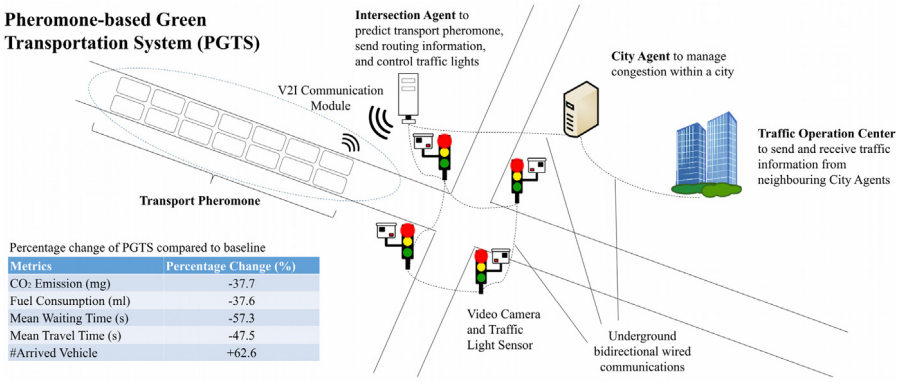

Percentage change of PGTS compared to baseline

Metrics	Percentage Change (%)
CO_2 Emission (mg)	-37.7
Fuel Consumption (ml)	-37.6
Mean Waiting Time (s)	-57.3
Mean Travel Time (s)	-47.5
#Arrived Vehicle	+62.6

ARTICLE INFO

Article history:
Received 30 November 2018
Received in revised form 12 April 2019
Accepted 6 May 2019
Available online 13 May 2019

Keywords:
Coordinated traffic light control
Multi-Agent
Pheromone
Green vehicle routing
Heterogeneous vehicle

ABSTRACT

Green transportation has been increasingly gaining attention in recent years. Existing pheromone-based traffic management frameworks were developed to reduce urban congestion by fusing traffic lights control strategies and vehicle routing schemes. Despite a significant reduction in traffic congestions, the greener aspects of transportation were not well investigated. In view of this, a Pheromone-based Green Transportation System (PGTS) is proposed to reduce Greenhouse Gas emissions and urban congestion in a three-step approach. First, traffic congestions are predicted based on the transport pheromone intensity of the target and adjacent upstream roads through an online epsilon-Support Vector Regression model. Second, a Coordinated Traffic Light Control (CTLC) strategy generates green wave scenario, dispersing heavy traffic on congested roads to the coordinated downstream paths. Third, a Cooperative Green Vehicle Routing (CGVR) takes a further leap by probabilistically rerouting upstream vehicles from entering the congested road, preventing the accumulation of vehicles that can lead to upstream congestion. Intuitively, the integration of CTLC and CGVR increases the chances that vehicles traversing multiple intersections with fewer frequencies of acceleration, effectively marking down fuel consumption. The proposed PGTS can be realized through a Pheromone-based Hierarchical Multi-Agent System (PHMAS). Based on Singapore traffic data, experimental results from a microscopic simulation SUMO show that the proposed PGTS outperforms other six approaches in reducing carbon dioxide emissions by 37.7%, fuel consumption by 37.6%, mean travel time by 47.5%, mean waiting time by 57.3%, and increasing number of arrived vehicles at designated destinations by 62.6%.

1. Introduction

Generally, Intelligent Transportation System (ITS) solutions to reduce traffic congestions are categorized into two broad

* Corresponding author.
E-mail addresses: Kian.Soon@monash.edu (K.L. Soon), Joanne.Lim@monash.edu (J.M.-Y. Lim), Rajendran.Parthiban@monash.edu (R. Parthiban).
https://doi.org/10.1016/j.asoc.2019.105486
1568-4946/

areas: (1) vehicle routing to direct vehicle away from traffic congestion [1–3], and (2) traffic light control to balance traffic flow [4–6]. The significance of green logistics has motivated the shift of research focus towards reducing the negative impacts on the environment and ecology [7]. Several green vehicle routing problems were addressed from the perspective of minimizing fuel consumption [8,9], carbon dioxide [10], and a mixture of them [11]. Meanwhile, traffic light control strategies were developed to minimize Greenhouse Gas (GHG) emissions through numerous swarm and evolutionary computing algorithms namely Particle Swarm Optimization [12], Bee Colony Optimization [4], Genetic Algorithm [5], and Ant Colony Optimization [13,14].

Recently, a pheromone-based traffic management framework was proposed to fuse traffic light control strategy and vehicle routing scheme to reduce urban congestion [15]. Designed as a Multi-Agent system, a minimal reduction in both carbon dioxide and fuel consumption was reported despite achieving a significant decrease in traffic congestion. It was revealed that the greener aspects of Multi-Agent transportation systems have not been well explored.

In view of this, a Pheromone-based Green Transportation System (PGTS) is proposed to reduce Greenhouse Gas emissions and urban congestion with threefold contributions: (1) the notion of pheromone intensity is introduced to detect the traffic density of a road network, followed by an online epsilon-Support Vector Regression model to forecast the occurrence of a congestion. The prediction of each target road is performed based on the transport pheromone intensity of its adjacent upstream road segments. (2) Once the traffic congestion is detected, the traffic lights on the upstream and downstream of the congested roads are coordinated to generate green wave scenarios via a Coordinated Traffic Light Control (CTLC) strategy. (3) To prevent the spread of congestion towards upstream roads, a further attempt is taken to probabilistically distribute upstream vehicles away from the congested road by using a Cooperative Green Vehicle Routing (CGVR) scheme. Looking from another perspective, CTLC disseminates the traffic to downstream paths while CGVR reduces the upstream congestion. The integration of CTLC and CGVR increases the chances of vehicles traversing multiple intersections with reduced frequency of acceleration. As fuel consumption is a function of acceleration and speed [16], a decrease in the frequency of acceleration reduces the fuel consumption. To tackle scalability issues, the proposed PGTS can be realized through a Pheromone-based Hierarchical Multi-Agent System (PHMAS) composed of City Agents, Intersection Agents, and Vehicle Agents.

There are some considerable differences between the proposed PGTS and existing pheromone-based approaches [15,17]. PGTS aims to reduce both transport emission and urban congestion considerably while the existing pheromone approaches balance traffic flow. In PGTS, the integration of CTLC and CGVR controls both downstream and upstream traffic of the congested roads, distributing vehicles to greener paths. The existing pheromone-based approaches adjust traffic signals and assign vehicles to paths with lower pheromone intensity to reduce travel time. Another noticeable difference is PGTS extends the existing pheromone-based approaches to consider both non-signalized intersections and signalized intersections with three color phases.

The rest of this paper is organized as follows. Section 2 reports the related work and their differences with the proposed PGTS. Section 3 details the Pheromone-based Hierarchical Multi-Agent System (PHMAS) and the PGTS scheme which comprises Pheromone-based Congestion Prediction (PCP), Coordinated Traffic Light Control (CTLC) strategy, and Cooperative Green Vehicle Routing (CGVR) scheme. Results and discussions are shown in Section 4 while conclusions are presented in Section 5.

2. Related work

To improve the environmental quality and human health, green vehicle routings and traffic light control strategies have been introduced to reduce transport emissions. In green vehicle routing, numerous swarm and evolutionary algorithms have been proposed to minimize the routing costs in terms of fuel consumption, carbon dioxide, and a combination of them. Particularly, a genetic algorithm based co-optimization method was proposed to provide the reference speed for drivers to reduce fuel consumption [18]. As it could be difficult for drivers to follow the desired reference speed for a specific duration, the proposed algorithm could be impractical in real-world applications. To promote practicality, varying speed constraint was incorporated to minimize fuel consumption through Particle Swarm Optimization with Greedy Mutation Operation [9]. Nevertheless, the behaviors of heterogeneous vehicles under varying speed constraints were not well investigated.

In addition to reducing fuel consumption, a Green Swarm routing scheme was developed to minimize carbon dioxide and promote sustainable cities [19]. Similarly, a Green Vehicle Routing and Scheduling Problem (GVRSP) was introduced to minimize carbon dioxide emissions via a Mixed Integer linear Programming (MIP) model for delivery and pickup plans [10]. In [11], both fuel consumption and carbon dioxide emissions were optimized using a Tabu Search based on the Comprehensive Modal Emission Model (CMEM). An examination of these strategies has revealed that these optimization techniques could lead to high computational time. It is also fascinating to fuse swam intelligence into green vehicle routing to reduce GHG emissions. Recently, a pheromone-based green vehicle routing has been proposed to assign vehicles to paths with multiple green signalized intersections to reduce transport emissions [20]. Furthermore, a Multi-Agent framework was incorporated into the Next Road Rerouting (NRR) scheme to distribute vehicles away from unexpected congestions [21], based on road occupancy, travel time, geographic distance to destination, and geographic closeness of congestion. Despite a significant decrease in travel time and traffic congestion, the investigation of the impacts of reducing GHG emission was still in the infancy stage.

Besides green vehicle routing, evolutionary computing has widely been adopted to optimize the signal settings in traffic lights. Ant Colony Optimization was employed to optimize the signal settings based on two kinds of artificial ant behaviors, specifically the response to pheromones for simulating user choice and the pressure of ant streams for resolving signal setting definition problem [13]. To reduce the level of pollutant emissions, Particle Swarm Optimization was proposed for optimal scheduling of traffic light timing programs in urban areas [12]. While these metaheuristic algorithms achieved substantial reduction in carbon monoxide and nitrogen oxides emissions, they imposed high computational time in searching for optimal solutions.

Cooperative traffic light control has become the recent focus to further mark down the transport emissions. In this case, vehicle passing rates in the signalized intersections were computed based on the registered vehicles at the current intersection, and unregistered vehicles at adjacent intersections, through the application of the Internet of Vehicles [22]. A concern was imposed on the feasibility of system in larger vehicular network, as assigning traffic phases based on lane basis could be computationally expensive. Another cooperative traffic light control strategy was proposed to compute the green time based on the queue length of the intersections [23]. Traffic phase of subsequent intersections was coordinated based on vehicle arrival at upstream intersections to generate green wave scenario, by

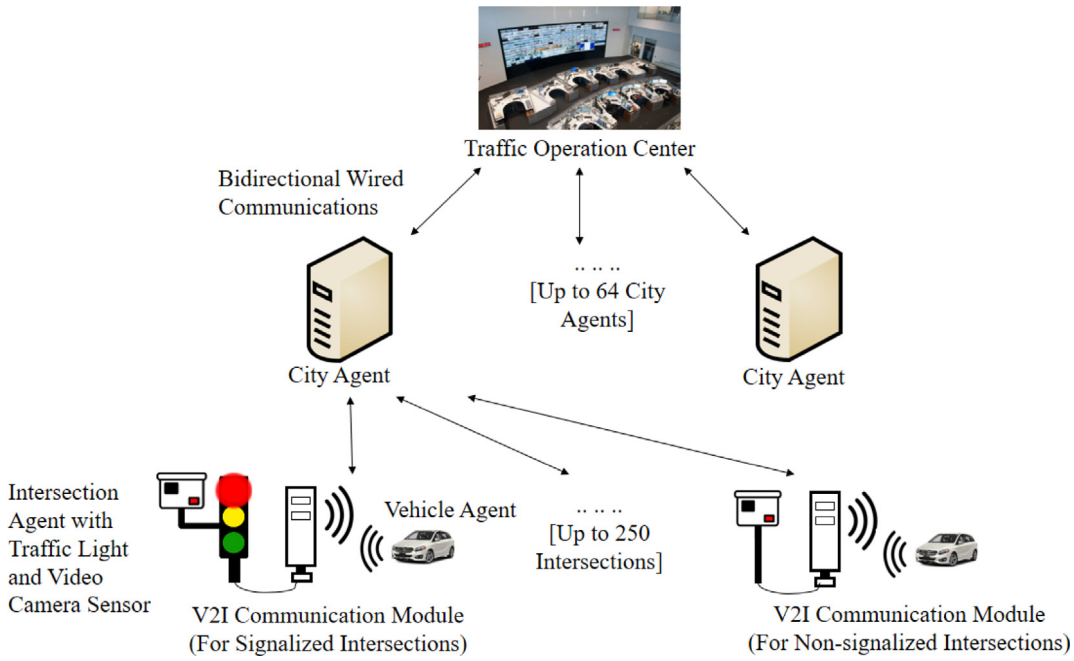

Fig. 1. Architecture of Pheromone-based Hierarchical Multi-Agent System (PHMAS).

exchanging traffic information between intersection agents and cooperative vehicles.

Advances in technologies have also motivated the implementation of Multi-Agent systems in traffic light control. A hierarchical multi-agent based traffic signaling model, along with Reinforcement Learning has been proposed to control traffic signal through the communication of Regional Agents (RAs), Intersection Agents (IAs) and Turning movement Agents (TAs) [24]. Different priority weights were imposed on each TA for the coordination of turning movements to generate green wave scenarios. One limitation is the exponential grow of the optimal setting for these priority weights of TA, specifically when the dimension of the system state grows with increased number of intersections.

As another worth noticing approach, pheromone-based Multi-Agent system was developed to bridge traffic light control strategies and vehicle routing schemes to reduce traffic congestions [15,17]. As the reduction of pollutant emission was relatively minimal, the motivation towards achieving green transportation has led to proposing a novel Pheromone-based Green Transportation System (PGTS) in this manuscript. Distinct from the existing pheromone-based frameworks [15,17], the integration of Cooperative Traffic Light Control (CTLC) (see Section 3.3) and Cooperative Green Vehicle Routing (CGVR) (see Section 3.4) effectively diverge the traffic on upstream and downstream of the congested roads to greener paths. The contribution is more pronounced when PGTS can be realized through a Pheromone-based Hierarchical Multi-Agent System (PHMAS) (see Section 3.1), which is an extension to the existing Sydney Coordinated Adaptive Traffic System (SCATS) model.

3. Pheromone-based Green Transportation System (PGTS)

Section 3.1 describes the architecture of Pheromone-based Hierarchical Multi-Agent System (PHMAS). In essence, Intersection Agents (IAs) model vehicles as ants through the notion of pheromone intensity to compute current density of road units (density pheromone) and future density of road units (future pheromone). In Pheromone-based Congestion Prediction (PCP), these two pheromone intensities are fused to predict short-term traffic density (transport pheromone), which determines the occurrence of a congestion (see Section 3.2). The upstream and downstream of the congested roads are coordinated to generate green wave scenario through Coordinated Traffic Light Control (CTLC) (see Section 3.3). To prevent upstream congestion, vehicles that have the intentions to traverse the congested roads are probabilistically rerouted to further mark down GHG emissions in Cooperative Green Vehicle Routing (CGVR) (see Section 3.4). It is worth noticing that CGVR does not forbid vehicles to enter the congested roads, as the congestion could be cleared by CTLC. The integration of CTLC and CGVR diverges traffic congestion to the downstream and reduce the impacts of its upstream congestions, respectively.

3.1. Pheromone-based Hierarchical Multi-Agent System (PHMAS)

As an extension of Sydney Coordinated Adaptive Traffic System (SCATS) [25], the proposed Pheromone-based Hierarchical Multi-Agent System (PHMAS) manages dynamic timing of traffic signals based on video camera sensors [26]. Inspired by the notion of pheromone intensity [15,17,20,27,28], PHMAS comprises the Traffic Operation Center (TOC), City Agent (CA), Intersection Agent (IA), and Vehicle Agent (VA), which are organized in a hierarchical manner. To facilitate the local communication between IAs and VAs, PHMAS employs Vehicle-to-Infrastructure (V2I) communication to enable the exchange of information including route intention, GPS speed, location data, predicted pheromone intensity and suggested paths for vehicles. V2I is less likely to suffer from Non-Line-Of-Sight (NLOS) communication issues, implying almost full communication coverage is achieved at each intersection to avoid signal blockage from the buildings [21]. The architecture of PHMAS is depicted in Fig. 1, with the respective roles and interactions of each hierarchy summarized in Table 1.

The proposed PHMAS is advantageous in three aspects: (1) PHMAS enables effective scaling of system to extremely large vehicular system as it operates in a hierarchical manner through the communication among City Agents, (2) Considering a bidirectional four-way intersection, each IA is responsible for managing the transport pheromone of four road links, which justifies the

Table 1
Roles and Interactions of the Traffic Operation Center and Multiple Agents.

Hierarchy	Roles	Interactions
Traffic Operation Center (TOC)	• Verify and notify the occurrence of congestion based on the predicted pheromone intensity (transport pheromone).	• Interact with CAs and IAs to obtain transport pheromone of the road links.
City Agent (CA)	• Update and manage transport pheromone intensity within a city.	• Inform TOC once the congestion is predicted.
Intersection Agent (IA)	• Obtain the number of vehicles via video camera sensors to compute current density of road units (density pheromone). • Compute future density of road units (future pheromone) based on the suggest route path, number of incoming and outgoing vehicles and traffic light phases information. • Fuse density pheromone and future pheromone to predict short-term traffic density of road units (transport pheromone) through epsilon-Support Vector Regression. • Compute a suggested route path for each VA according to the route intention (Origin–Destination Pair). IA detects the new location of VA (i.e. through GPS) if VA does not follow the suggested route path. A new path is then re-computed based on transport pheromone.	• Communicate with VA to provide the suggested path and update transport pheromone of each road unit. • Interact with neighboring IAs to obtain upstream and downstream traffic light phases and durations. • Obtain incoming and outgoing vehicle numbers from sensors. • Communicate with neighboring CAs to obtain transport pheromone from neighboring city if VAs intend to travel from current city to neighboring city.
Vehicle Agent (VA)	• Each VA is embedded with a wireless sensor. • Deposit pheromone intensity and report route intention to IA. • Update current location (i.e. from GPS) to IA.	• Coordinate with IAs to obtain real-time transport pheromone intensities and the suggested route path.

efficiency PGTS, and (3) PHMAS is robust even in the event of system failure, specifically during power outage within a city, as other agents outside the affected cities can still operate normally through local communication [6].

3.2. Pheromone-based Congestion Prediction (PCP)

As the first step in PHMAS, PCP performs short-term traffic forecasting to predict the occurrence of congestion. Recent pheromone-based prediction models [15,17] performed prediction by considering signalized intersections, with only green and red phases. To bridge this gap, PCP takes a further leap to forecast congestion for both non-signalized intersections and signalized intersections with all three color phases.

In PCP, the density pheromone $T_d(p,t)$ and future pheromone $T_f(p,t+1)$ are defined to represent current and future traffic density on a particular road p, respectively. Density pheromone is deposited when vehicles traverse on road p, and collected by Intersection Agents (IAs) as defined below:

$$T_t\,(p,\,t) = \frac{N\,(p,\,t)\;\times L_{veh}}{L\,(p)\;\times\;N_{lane}\,(p)},\; 0 \le T_d(p,\,t) \le 1 \tag{1}$$

where $N(p,t)$ represents the number of vehicles on road p in time (t-1, t], L_{veh} is the mean vehicle length in meter, $L(p)$ is the length of road p in meter and $N_{lane}(p)$ is the number of lanes of road p. A high density pheromone intensity represents high vehicle numbers on road p in time t, and vice versa. Future pheromone is defined by replacing $N(p,t)$ with $N_{in}(p,t+1)$- $N_{out}(p,t+1)$ to estimate near future traffic density of road p, as follows:

$$T_f\,(p,\,t+1) = \frac{[N_{in}\,(p,\,t+1) - N_{out}\,(p,\,t+1)] \times L_{veh}}{L\,(p) \times N_{lane}\,(p)},\quad T_f(p,\,t+1) \epsilon \mathbf{R} \tag{2}$$

where $N_{in}(p,t+1)$ and $N_{out}(p,t+1)$ represent the incoming and outgoing vehicle volume flowing from neighboring roads $p' \epsilon\, p_{nei}$ to road p in time $(t,t+1]$, respectively. A positive value in $T_f(p,t+1)$ implies a net incoming vehicle volume flowing from neighboring road p' to road p, and vice versa. The incoming vehicle count, $N_{in}(p,t+1)$ that considers four different sub-traffic scenarios is defined below:

$$N_{in}\,(p,\,t+1) = \begin{cases} 0, \quad red\ phase\,,\ T_{step} \le T_{remain\_red}\,, & (i) \\ \sum\limits_{p' \in p_{nei}} f_{free}\,(p') \times (T_{step} - T_{remain\_red}) x \rho_{in}, & \\ \quad red\ phase\,,\ T_{step} > T_{remain\_red}\,, & (ii) \\ \sum\limits_{p' \in p_{nei}} f_{avg}\,(p') \times T_{step} \times \rho_{in}, & \\ \quad yellow\ phase\,,\ T_{step} \le T_{remain\_yellow}\,, & (iii) \\ \sum\limits_{p' \in p_{nei}} f_{avg}\,(p') \times T_y\,(p') \times \rho_{in}, & \\ \quad yellow\ phase\,,\ T_{step} > T_{remain\_yellow}\,, & (iv) \\ \sum\limits_{p' \in p_{nei}} f_{free}\,(p') \times T_{step} \times \rho_{in}, & \\ \quad green\ phase\,,\ T_{step} \le T_{remain\_green}\,, & (v) \\ \sum\limits_{p' \in p_{nei}} f_{free}\,(p') \times T_g\,(p') \times \rho_{in}, & \\ \quad green\ phase,\ T_{step} > T_{remain\_green}\,, & (vi) \\ \sum\limits_{p' \in p_{nei}} f_{free}\,(p') \times T_{step} \times \rho_{in}, & \\ \quad no\ traffic\ light\,, & (vii) \end{cases} \tag{3}$$

$$\text{with } 0 \le \rho_{in} \le 1, f_{free}, f_{avg}, T_{step}, T_{remain\_red}, N_{in}(p,\,t+1) \in \mathbf{R}^{+} \tag{3}$$

where $f_{free}(p') = \frac{V_{free}(p')N(p',t)}{L(p')}$, is the estimated flow rate on road p' and $f_{avg}(p') = \frac{V_{avg}(p')N(p',t)}{L(p')}$, is the estimated average flow rate on road p', wherein $V_{free}(p')$ is the free speed of road p', $V_{avg}(p')$ is the average speed of road p', $N(p',t)$ is the number of vehicles on neighboring road p' and $L(p')$ is the length of neighboring

road p'; T_{step} represents time step; T_{remain_red} is the remaining red light duration; $T_y(p')$ is the total yellow phase duration; $T_g(p')$ is the total green phase duration; ρ_{in} is the proportion of vehicle number that is able to pass the stop-line in the remaining traffic light duration, which is proposed in Eq. (4):

$$\rho_{in} = \frac{s\left(p'\right)}{N_{intention}\left(p'\right)}, 0 \leq \rho_{in} \leq 1 \tag{4}$$

where $N_{intention}(p')$ represents a total number of vehicles having the intention to travel from p' to p, $s(p')$ represents the number of vehicles that can pass through the stop-line in remaining traffic light duration from p' to p. $N_{out}(p,t+1)$ in Eq. (2) follows similar formulation as defined in Eq. (3) and Eq. (4), by just removing the summation and replacing neighboring road p' with p.

The proposed future pheromone intensity describes the dynamic computation of $N_{in}(p,t+1)$ and $N_{out}(p,t+1)$ based on traffic light states and durations for signalized intersections, and T_{step} for non-signalized intersections. Both density pheromone and future pheromone intensities are fused through epsilon-Support Vector Regression (εSVR) to perform short-term traffic prediction. In essence, the εSVR in LIBSVM [29] is employed, with the training instances $\{(\boldsymbol{x_1},y_1),\ldots,(\boldsymbol{x_t},y_t)\}$, where $\boldsymbol{x_t} \in \mathbf{R}^2$ is a feature vector and $y_t \in \mathbf{R}^1$ is the target output, as follows:

$$\boldsymbol{x_t} = \left(T_t\left(p, t-1\right), T_f\left(p, t\right)\right) \tag{5}$$

$$y_t = T\left(p, t\right) = T_t\left(p, t\right) \tag{6}$$

After obtaining the pheromone information in (5) and (6) in time $(t-1,t]$, the transport pheromone is predicted as follows:

$$T(p, t+1) = \sum_{i=1}^{l} \left(-\boldsymbol{\alpha} + \boldsymbol{\alpha^*}\right) K\left(\boldsymbol{x_i}, \boldsymbol{x_j}\right) + b \tag{7}$$

where α,α^* are the dual variables, K is the RFB Kernel, b is the bias, and the training set includes $t = 100$ instances. The proposed PCP is distinct from the existing pheromone models [15,17,27] in two aspects. First, the PCP is an online εSVR model that dynamically trains the latest 100 training samples (moving time window of 100 instances) to forecast stochastic traffic conditions. Second, future pheromone is a new notion developed to describe future traffic density on both non-signalized intersections and signalized intersections.

3.3. Coordinated Traffic Light Control (CTLC)

Once the transport pheromone intensities of all roads are predicted by PCP, the number of congested roads, $\#Rd_{Con}(t)$ is determined through the dynamic congestion threshold parameter, $\delta_d(t)$. For each time step t, the process commences by initializing the parameter $\delta_d(t)$ to δ_{heavy}, which aims to determine the initial number of congested roads, $\#Rd_{ConInitial}(t)$ in a vehicular system. The system is heavily congested if $\#Rd_{ConInitial}(t)$ exceeds the threshold number of the congested roads ($\#Rd_{ConThreshold}$), and vice versa. $\#Rd_{ConThreshold}$ is the product of percentage of roads in a vehicular system that is considered as congested ($\%Rd_{Con}$) and total number of roads ($\#Total_{Rd}$). $\delta_d(t)$ is then updated via on Eq. (8) based on the congestion level of the vehicular system, being Eq. (8)(i) if light congestion and Eq. (8)(ii) if heavy congestion. The proposed $\delta_d(t)$ follows the formulation as follows:

$$\delta_d(t) = \begin{cases} \dfrac{\delta_{heavy} - \delta_{light}}{\sqrt{\#Rd_{ConThreshold}}} \sqrt{\#Rd_{ConInitial}(t)} + \delta_{light}, & \\ \qquad \delta_{light} < \delta_d(t) < \delta_{heavy} & (i) \\ \delta_{heavy}, \quad \delta_d(t) \geq \delta_{heavy} & (ii) \end{cases} \tag{8}$$

where δ_{heavy} is the transport pheromone intensity when a road p is considered heavily congested, and δ_{light} is the transport pheromone intensity when a road p is considered lightly congested. Also notice that the minimum value of $\delta_d(t)$ is δ_{light} while the maximum value of $\delta_d(t)$ is δ_{heavy}. The $\#Rd_{Con}(t)$ is then refined based on the new $\delta_d(t)$ in CTLC. Different from the existing pheromone approaches [15,17], the main role of $\delta_d(t)$ aims to coordinate traffic lights in both lightly (Eq. 8(i)) and heavily congested system (Eq. (8)(ii)), to further reduce GHG emission and fuel consumption. The coordination is performed even in the case of light congestion to prevent further accumulation of vehicles, which could lead to heavy congestion in next few time steps. CTLC is not triggered when there is no congestion in a vehicular system.

As traffic congestion exhibits spatial–temporal characteristics [30], the congestion is usually initiated at one or more segments before spreading to other segments, leading to regional congestion [31]. Controlling traffic lights on the upstream and downstream of the congested road is therefore effective to reduce traffic congestion. Once $\#Rd_{Con}(t)$ is determined, the corresponding r-hop upstream and m-hop downstream of the congested road are coordinated to generate green wave scenario and reduce traffic congestion. The coordination is performed by each IA, which interact with neighboring IAs to dynamically receive, compute and set green traffic phases and durations. It is worth noticing that CTLC coordinates r-hop upstream and m-hop downstream traffic lights through local communication among IAs. To offer better insights, Fig. 2(a) and (b) illustrate the process of CTLC: (1) Coordination of the upstream and downstream of the heaviest congested road, and (2) Coordination of the upstream and downstream of the all subsequent roads.

Depicted in Fig. 2(a), the level of congestion decreases in the order of $p_{13} > p_8 > p_{10}$ based on the transport pheromone intensity. As CTLC prioritizes the heaviest congestion, the traffic lights on p_{13} and both of its r-hop upstream and m-hop downstream road segments are coordinated to generate green wave scenario. As the parameter r is 1 and m is 3, the coordinated paths are listed as follows:

C1: $p'_2 >> p_{13} >> p_1 >> p_2 >> p_3$
C2: $p'_2 >> p_{13} >> p_1 >> p_2 >> p_6$
C3: $p'_2 >> p_{13} >> p_4 >> p_7 >> p_{11}$

As the traffic lights are set to green for these coordinated paths, vehicles have higher chances to traverse multiple intersections with fewer frequency of acceleration. As fuel consumption is a function of acceleration and speed [16], CTLC has the added value of reducing GHG emissions. The distribution of vehicles to these green-traffic-light paths disseminates the traffic congestion on p_{13} to its downstream paths. To further reduce pollutant emissions, the traffic light of the corresponding direct upstream of p_{13} is set to green. In essence, CTLC disperses traffic on the congested roads to the m-hop downstream paths.

Upon completion of the coordination of the heaviest congested road, CTLC searches the next congested road to check if its r-hop upstream and m-hop downstream have been coordinated previously. In Fig. 2(b), traffic light *T8* has been coordinated by the downstream of p_{13} (path *C2*), the traffic lights of p_8 and its corresponding upstream and downstream roads are not coordinated. The subsequent congested road is detected at p_{10}, IAs search the feasible paths as *TL10* has not been coordinated previously. As the traffic light of the direct upstream road has been coordinated (path *C3*), the feasible m-hop downstream paths of p_{10} is shown as follows:

C4: $p_{10} >> p_{16} >> p_{19} >> p_{23}$
C5: $p_{10} >> p_{16} >> p_{19} >> p_{20}$
C6: $p_{10} >> p_{13} >> p_{14} >> p_{15}$
C7: $p_{10} >> p_{13} >> p_{17} >> p_{20}$
C8: $p_{10} >> p_{13} >> p_{17} >> p_{23}$

As the traffic light of *T11* has been coordinated by the downstream of p_{13} (path *C3*), only path C4 and C5 are coordinated to

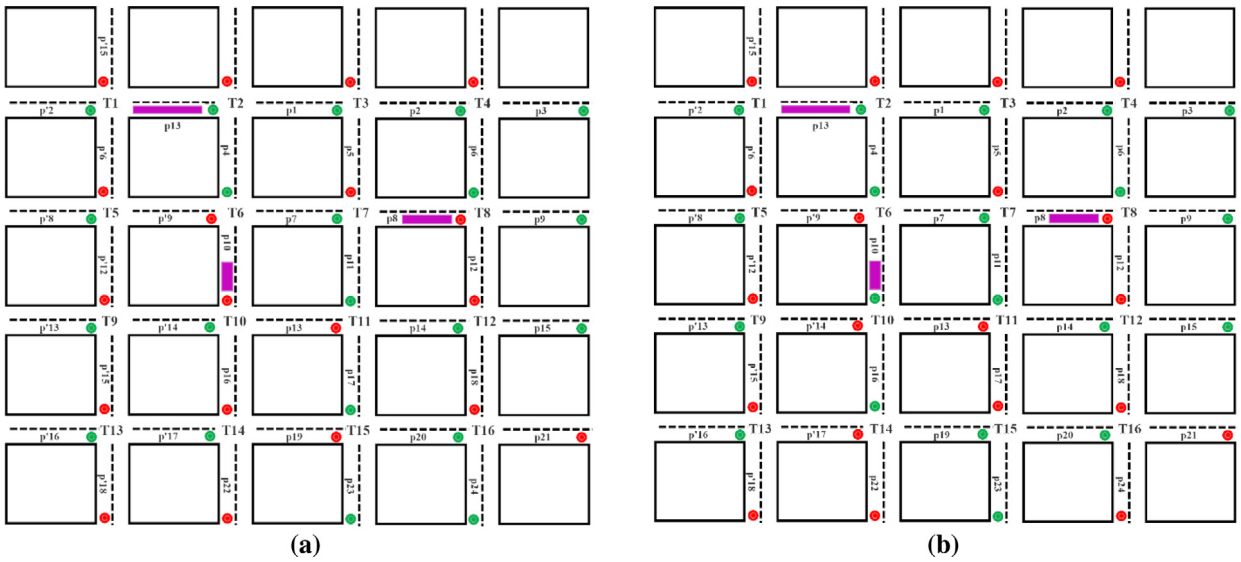

Fig. 2. (a) Coordination of upstream and downstream roads of the heaviest congested road (p_{13}); (b) Coordination of upstream and downstream roads of the all subsequent congested roads.

further promote green transportation. CTLC algorithm stops when all the subsequent congested roads are coordinated. Algorithm 1 and 2 depict the CTLC and *SetGreenPhase* pseudo-codes. The *SetGreenPhase* algorithm forms the part of the CTLC algorithm to set the traffic lights to green if the signalized intersection has not been coordinated.

Algorithm 1 coordinates the traffic lights on the r-hop upstream and m-hop downstream of all congested roads. Line 1 checks if there is any $\#Rd_{Con}(t)$ in the vehicular system. If $\#Rd_{Con}(t)$ is present, line 2 initializes the $state_{stopcoordinate}$ to 1 while line 3 finds the congested road with the maximum transport pheromone intensity *T(p,t+1)*. Lines 4–9 check if the congested road leads to a non-signalized intersection. Specifically, line 5 removes the checked p from $Rd_{Con}(t)$ if non-signalized intersection is identified at p. If p leads to a signalized-intersection, line 7 sets the traffic light to green with the duration of $t_{coordinate}$ via *SetGreenPhase* (see Algorithm 2). After coordinating the traffic lights, line 8 removes the checked p from $Rd_{Con}(t)$ and line 9 sets $state_{stopcoordinate}$ to 0, indicating there is a need to coordinate its r-hop upstream and m-hop downstream road segments. Line 10 enables the coordination of the traffic lights on the upstream and downstream of p, only if the traffic light of road p has been coordinated in lines 7–9. Lines 11–17 perform similar function as in lines 3–9, by just replacing p with p_{up} and searching for r-hop upstream roads ($P_{upstream}$). Similarly, lines 18–24 perform the function as in lines 3–9, with the replacement of p with p_{down} and searching for m-hop downstream roads ($P_{downstream}$).

The main objective of algorithm 2 aims to set green phase to traffic lights on road p, based on its current traffic phase and the corresponding competing roads connecting to the same signalized intersections. Line 1 checks if the traffic light has been coordinated previously. Line 3 sets the green duration of TL_p to $t_{coordinate}$ when line 2 detects the green $phase.TL_p$. If line 4 detects yellow phase at TL_p, line 5 sets $phase.TL_p$ to green with its corresponding duration $t_g.TL_p$ to $t_{coordinate}$. When the $phase.TL_p$ is red, lines 8–15 check the traffic phases on the competing roads connecting to the same intersection. Particularly, as green $phase.TL_{p\_opposite}$ is detected in line 8, its phase is set to yellow to allow vehicles to decelerate. Line 10 then sets $phase.TL_p$ to green and $t_g.TL_p$ to $t_{coordinate}$ after the competing $phase.TL_{p\_opposite}$ turns red. If yellow $phase.TL_{p\_opposite}$ is detected in line 11, the $phase.TL_p$ is set to green and $t_g.TL_p$ to $t_{coordinate}$ after the competing $phase.TL_{p\_opposite}$ turns red. As line 13 detects red $phase.TL_{p\_opposite}$, the $phase.TL_p$ is set to green with its corresponding $t_g.TL_p$ to $t_{coordinate}$, allowing vehicles on p to traverse multiple intersections.

3.4. Cooperative Green Vehicle Routing (CGVR)

To prevent over routing, CGVR mainly selects vehicles on r-hop upstream, which have the intention to enter the congested road. After the vehicle selection, the number of feasible paths is computed via the proposed dynamic k-shortest path (dkSP), based on the transport pheromone intensity of the congested road. In this case, d out of k paths are assigned to vehicles having the intention to traverse the congested road with $\delta_d \leq T_{con} \leq 1$. In other words, a maximum of k paths is selected when T_{con} is one. The proposed dkSP takes the following formulation:

$$d = k \exp\left(T_{con}^{\gamma} - 1\right), \delta_d \leq T_{con} \leq 1 \tag{9}$$

where k is the maximum number of paths, T_{con} is the transport pheromone intensity of a congested road, γ is the relative importance of T_{con}.

Distinct from the existing pheromone-based approaches [15, 17] which adopt the conventional kSP, the main role of dkSP targets to compute the number of paths in accordance to global distance and number of intersections. A shorter distance path with higher number of intersections leads to higher frequency of acceleration, unnecessarily increasing fuel consumption. In view of this, dkSP takes a further leap to consider both static traffic information of global distance and number of intersections, which are preloaded into the vehicular system.

After computing the feasible paths, a modified variant of Logit Probabilistic Equation [32,33] is proposed to distribute vehicles based on the mean road speed and transport pheromone intensity on the m-hop downstream roads. Each vehicle v_j probabilistically chooses path $q \epsilon d$ based on Eq. (10) as follows:

$$P_q^j = \frac{\exp(-w\ T_q^m \exp(\beta \overline{v_q^m}))}{\sum_{q=1}^{d} \exp(-w\ T_q^m \exp(\beta \overline{v_q^m}))} \tag{10}$$

where w is the relative importance of the routing cost of $T_q^m \exp(\beta \overline{v_q^m})$, d is the dynamic shortest paths computed via Eq. (9), where T_q^m is the transport pheromone intensity on mth-hop downstream road of q path, $\overline{v_q^m}$ is the mean speed road on mth-hop downstream road of q path, and β is the weight of $\overline{v_q^m}$.

Algorithm 1: Coordinated Traffic Light Control

Input: $\#Rd_{Con}(t)$, number of congested roads at time t; TL_p, traffic light on road p;
$phase.TL_p$, current phase of traffic lights on road p;
$t_g.TL_p$, green phase duration of traffic lights on road p;
$t_{coordinate}$, duration for traffic light coordination;
Output: $phase.TL_p$, current phase of traffic lights on road p;
$t_g.TL_p$, green phase duration of traffic lights on road p;

while $\#Rd_{Con}(t) > 0$ **do**
  Set $state_{stopcoordinate} = 1$
  Find road $p \in Rd_{Con}(t)$ with maximum $T(p,t+1)$
  if $p \in Rd_{Con}(t)$ leads to a non-signalized intersection **do**
    Remove the checked $Rd_{Con}(t) = Rd_{Con}(t) - p$
  else
    $SetGreenPhase(p, Rd_{Con}(t), phase.TL_p, t_g.TL_p)$
    Remove the checked $Rd_{Con}(t) = Rd_{Con}(t) - p$
    Set $state_{stopcoordinate} = 0$
  if $state_{stopcoordinate} == 0$
    Get r-hop upstream road $P_{upstream}$ of $p \in Rd_{Con}(t)$
    for $p_{up} \in P_{upstream}$ **do**
      if $p_{up} \in P_{upstream}$ leads to a non-signalized intersection **do**
        Remove the checked $Rd_{Con}(t) = Rd_{Con}(t) - p_{up}$
      else
        $SetGreenPhase\ (p_{up}, Rd_{Con}(t), phase.TL_{pup}, t_g.TL_{pup})$
        Remove the checked $Rd_{Con}(t) = Rd_{Con}(t) - p_{up}$
    Get m-hop downstream road $P_{downstream}$ of $p \in Rd_{Con}(t)$
    for $p_{down} \in P_{downstream}$ **do**
      if $p_{down} \in P_{downstream}$ leads to a non-signalized intersection **do**
        Remove the checked $Rd_{Con}(t) = Rd_{Con}(t) - p_{down}$
      else
        $SetGreenPhase\ (p_{down}, Rd_{Con}(t), phase.TL_{pdown}, t_g.TL_{pdown})$
        Remove the checked $Rd_{Con}(t) = Rd_{Con}(t) - p_{down}$

Algorithm 2: SetGreenPhase

Input: p, a particular road p; $Rd_{Con}(t)$, congested roads; TL_p, traffic light on road p;
$phase.TL_p$, current phase of traffic lights on road p;
$t_g.TL_p$, green phase duration of traffic lights on road p;
Output: $phase.TL_p$, current phase of traffic lights on road p;
$t_g.TL_p$, green phase duration of traffic lights on road p;

if TL_p has not been coordinated **do**
  if $phase.TL_p ==$ 'green' **do**
    Set $t_g.TL_p = t_{coordinate}$
  elseif $phase.TL_p ==$ 'yellow'
    Set $phase.TL_p ==$ 'green'
    Set $t_g.TL_p = t_{coordinate}$
  elseif $phase.TL_p ==$ 'red'
    if $phase.TL_{p\_opposite} ==$ 'green'
      Set $phase.TL_{p\_opposite} ==$ 'yellow'
      Set $phase.TL_p ==$ 'green' and $t_g.TL_p = t_{coordinate}$ after $phase.TL_{p\_opposite}$ turns 'red'
    elseif $phase.TL_{p\_opposite} ==$ 'yellow'
      Set $phase.TL_p ==$ 'green' and $t_g.TL_p = t_{coordinate}$ after $phase.TL_{p\_opposite}$ turns 'red'
    elseif $phase.TL_{p\_opposite} ==$ 'red'
      Set $phase.TL_p ==$ 'green'
      Set $t_g.TL_p = t_{coordinate}$

The Logit Probabilistic Equation is computed based on m-hop downstream traffic information through local communication among IAs. The need of computing global dynamic information on all road segments which always leads to a centralized system [2,34] is alleviated in CGVR. Intuitively, CGVR scheme offers another alternative to following optimal speed as it can be difficult for drivers to follow a particular reference speed for a specific duration [18].

To offer clearer insights, Fig. 3 depicts the process of path selection through the modified Logit Probabilistic Equation. As the heaviest congestion occurs at p_0, the vehicles on the corresponding r-hop upstream are triggered for routing. With $m = 3$,

vehicles on p_{18} are rerouted to the feasible paths (*VPs*) computed via *dk*SP as follows:

VP1: p_{18} >> p_0 >> p_8 >> p_9
VP2: p_{18} >> p_0 >> p_2 >> p_6
VP3: p_{18} >> p_1 >> p_5 >> p_6
VP4: p_{18} >> p_1 >> p_{11} >> p_{15}

In CGVR, higher probability is allocated to select paths with higher mean road speed and lower transport pheromone intensity, indicating the path is free of traffic congestion. As higher transport pheromone intensities and lower mean road speed are depicted on p_0 and p_{11}, *VP3* has higher probability to be selected for vehicle assignment. Realized that Eq. (10) allows other paths to be selected for routing yet with lower probability, as the congestion could be cleared through the proposed effective CTLC (see Section 3.3).

Algorithm 3 shows the pseudo-code for the cooperative vehicle routing.

Once the number of congested roads ($\#Rd_{Con}$) are computed, lines 2–15 recursively assign a greener route for each vehicle in each OD pair based on global distance, number of intersections, transport pheromone intensity and mean travel speed of *m*-hop downstream road segments. Particularly, line 2 searches the road $p \epsilon Rd_{Con}$ with maximum *T(p, t+1)* while line 4 finds neighboring roads $p' \epsilon P_{nei}$ for each congested road $p \epsilon Rd_{Con}$. For each neighboring road $p' \epsilon P_{nei}$, line 5 obtains vehicle $j \epsilon V_{int}$ having intention to traverse $p \epsilon Rd_{Con}$ whereas line 6 groups these vehicles V_{int} into OD pairs. Line 8 computes dynamic *k*-shortest paths based on global distance and #intersections for each OD pair. Line 10 ranks the vehicles based on fuel consumption model, f_i. As different vehicle types have different fuel consumption model [16], vehicles with higher ranking are prioritized and rerouted first. Line 11 computes the probability of vehicles on route selection while line 12 distributes the vehicles accordingly. Line 13 updates future pheromone $T_f(p,t+1)$ while line 14 removes the checked road P_{con}. In line 15, new transport pheromone intensities are updated in road network *H*.

3.5. Interactions between CTLC and CGVR

To achieve optimal performance in PGTS, congestion is predicted via PCP to determine the need of CTLC and CGVR. To offer in-depth insights, Fig. 4 depicts the integration of CTLC and CGVR to promote green transportation. Initially, PCP detects the congestion occurring on p_{13} and p_1. As the priority is given to p_{13}, the computed feasible paths through the integration of CTLC and CGVR is listed as follows:

TR1: p'_2 >> p'_6 >> p'_{12} >> p'_{13}
TR2: p'_2 >> p'_6 >> p'_{12} >> p'_{14}
TR3: p'_2 >> p_{13} >> p_1 >> p_2
TR4: p'_2 >> p_{13} >> p_4 >> p_7

CTLC disperses the heaviest traffic congestion road p_{13} to the *m*-hop downstream (paths *TR3-4*) through local traffic signaling coordination to generate green wave scenario. In addition to controlling downstream traffic, attempts are made to prevent the accumulation of vehicles on the congested road that can lead to upstream congestions. Particularly, CGVR assigns *r*-hop upstream vehicles to greener paths (*TR1-2*) with lower pheromone intensity and higher mean road speed. This integration disseminates the upstream and downstream traffic to greener paths to reduce GHG emissions.

CTLC searches for the subsequent congested road, which occurs on p_1. CTLC is not triggered as the traffic light on p_1 has been coordinated through *TR3*. CGVR reroutes vehicles on its *r*-hop upstream (p_{13} for instance) through dkSP, with the following feasible paths:

TR5: p_{13} >> p_4 >> p_7 >> p_{11}
TR6: p_{13} >> p_4 >> p_7 >> p_8
TR7: p_{13} >> p_1 >> p_2 >> p_3

As the subsequent congestion occurs on the coordinated path, CGVR takes the advantage to distribute vehicles on p_{13} to these paths (*TR5-6*). Looking from another perspective, CGVR effectively avoids vehicle assignment to *TR7*, as distributing vehicles this path would worsen the traffic congestion. To summarize, CTLC controls downstream traffic signaling time while CGVR disseminates upstream traffic.

4. Results and discussion

The comparison between the proposed PGTS and other existing pheromone-based techniques is summarized in Table 2. To promote practicality, three additional robustness tests of PGTS are evaluated in terms of compliance rate, penetration rate, and available traffic data rate.

4.1. Experimental setup

The experiment is conducted with the objective of evaluating the performance of the proposed PGTS and existing pheromone-based approaches in terms of fuel consumption, carbon dioxide emission, mean vehicle waiting time, the number of arrived vehicles and mean travel time. Forty experiments are conducted via the platform of Simulation of Urban Mobility (SUMO) [35], which is an open source microscopic traffic simulator. Fig. 5 depicts the Singapore Cityhall map, which is downloaded from the OpenStreetMap to represent the downtown of Singapore. Singapore traffic data consisting of four vehicle types from March 2018 Singapore's DataMall [36] is employed with a Poisson distribution to represent realistic fluctuation of rush hour traffic behavior in arrival pattern [23]. Numerous commands in Traci library [37] are employed to manage routing and traffic lights control in MATLAB. Table 3 depicts the vehicle attributes, and the corresponding PGTS configurations are also illustrated as follows:

(1) 4000 vehicles are employed in an hour simulation with randomly generated trips.
(2) The parameters of ε-SVR in LIBSVM [29]: $C = 10$, RBF kernel with $\gamma = 0.15$, and $\varepsilon = 0.0001$.
(3) Dynamic threshold parameters: $\delta_{heavy} = 0.4$, $\delta_{light} = 0.25$, and $\%Rd_{Con} = 0.04$
(4) Upstream and downstream road segment parameters: $m = r = 3$
(5) Vehicles arriving destination will park and do not occupy the road.
(6) The parameters of dksp: $k = 6.5$ and $\alpha = 1$

4.2. PGTS Evaluation and analysis

Figs. 6–9 depict the comparison of all approaches in terms of fuel consumption, carbon dioxide emission, number of congested roads, and mean travel time. At the first glance, all the proposed CTCL, CGVR and PGTS strategies outperform their respective TLC-CDT, Rerouting-τ, and Combination-τ schemes for all performance metrics. A closer investigation of traffic light control strategies shows a relatively significant reduction of carbon dioxide emission (15.1%) and fuel consumption (14.8%) in CTCL, while a minimal decrease of both transport emissions (4.8%) in TLC-CDT at 3600 s. CTCL coordinates upstream and downstream traffic to generate green wave scenario, leading to a significant reduction of GHG emissions. On the contrary, TLC-CDT balances traffic loads by considering the competing relationship with neighboring roads. In other words, CTLC disperses congestion into multi-hop downstream road segments while TLC-CDT disseminates traffic into

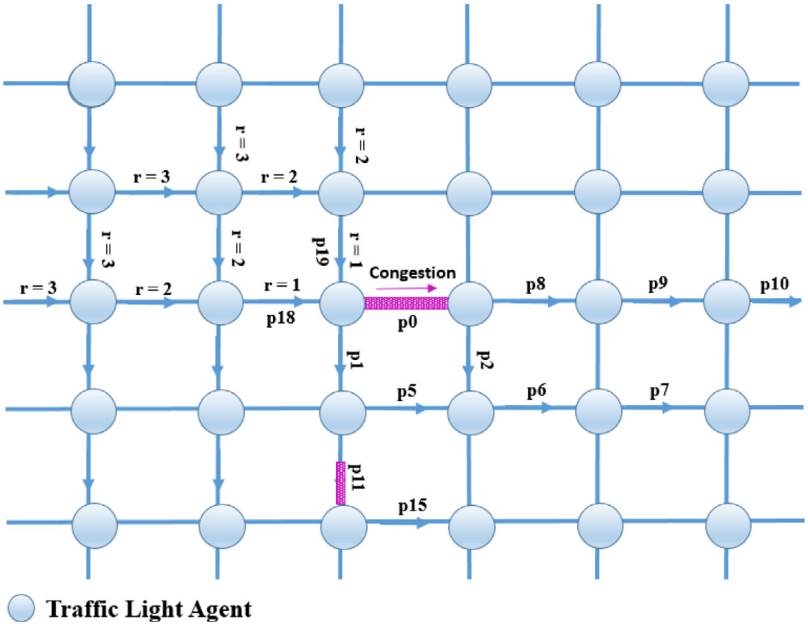

Fig. 3. Path assignment methodology in CGVR.

Algorithm 3: Cooperative Green Vehicle Routing

Input:
H, road network
Rd_{Con}, congested roads
t, current timestep
d, number of dynamic shortest path
m, number of downstream road segments
Output:
Road network with updated pheromone, H

while $\#Rd_{Con} > 0$ **do**
  Find road $p \epsilon Rd_{Con}$ with maximum $T(p,t+1)$
  Get neighboring roads $p' \epsilon P_{nei}$ connected to road p
  for $p' \epsilon P_{nei}$ **do**
    Obtain vehicles $j \epsilon V_{int}$ having intention to traverse p based on r-hop upstream roads
    Group $j \epsilon V_{int}$ with the same OD Pair
    for $od \epsilon OD_{nei}$ **do**
      Select d-shortest paths based on global distance and #intersections
      for $j \epsilon V_{int}$ **do**
        Prioritize vehicle j based on fuel consumption model, f_i
        Compute probability P_q^j for each vehicle $j \epsilon V_{int}$ *on* each $q \epsilon d$ path based on transport pheromone intensity and mean road speed m-hop downstream links
        Distribute vehicles to one of the d-paths according to P_q^j
    Update pheromone $T_f(p',t+1)$
  Remove the congested road p from P_{con}
Update and output road network with new transport pheromone on H

the next downstream road segment. A 14.0% decrease in mean travel time further attests the effectiveness of CTCL in diverging the heavy traffic on the predicted congested roads into multi-hop downstream, as compared to the baseline.

As for vehicle routing strategies, Rerouting-τ exhibits a respective decrease in both CO_2 emission and fuel consumption by 16.4% and 16.6%, while CGVR experiences a relatively substantial reduction of these emissions by 24%. As Rerouting-τ reroutes vehicles solely based on lower pheromone intensity to reduce congestion, the frequency of acceleration within the path is not well explored. To bridge this gap, CGVR employs an additional mean road speed parameter to indicate the traffic flow of the selected path. This parameter is critical as the increase in transport pheromone intensity is proportional to the vehicle number on the path, yet inversely proportional to its mean road speed [38]. In fact, this added parameter is inspired by the notion of evaporation rate, whereby the reduction of transport pheromone trails is proportional to the mean road speed. Hence, the traffic on a path with high transport pheromone intensity is fluent even if the evaporation rate (mean road speed) is high. CGVR takes this advantage to assign vehicles to paths with higher evaporation rate and lower transport pheromone intensity to reduce the frequency

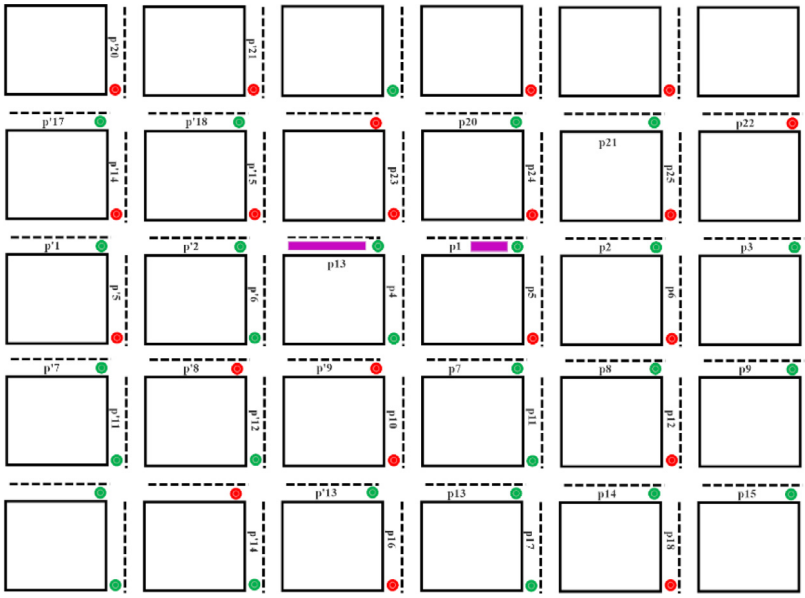

Fig. 4. Interactions between CTLC and CGVR.

Table 2
Comparison of PGTS and other pheromone-based techniques.

#	Approaches	Vehicle routing methodology			Traffic light control methodology
		Path assignment method	Static information	Dynamic information	
1	Baseline, without vehicle routing and traffic light control	NA	NA	NA	NA
2	TLC-CDT, Traffic Light Control Considering Downstream Traffic [15]	NA	NA	NA	Competing Relationship between neighboring roads
3	CTLC, Coordinated Traffic Light Control	NA	NA	NA	Coordination of traffic lights based on transport pheromone
4	Rerouting-τ, pheromone-based rerouting approach [15]	kSP	Global distance	Pheromone intensity	NA
5	CGVR, Cooperative Green Vehicle Routing	dkSP	Global distance + #intersections	Transport pheromone + mean road speed	NA
6	Combination-τ, combination of TLC-CDT and Rerouting [15]	kSP	Global distance	Pheromone intensity	Competing Relationship between neighboring roads
7	PGTS, Pheromone-based Green Transportation System, combination of CTLC and CGVR	dkSP	Global distance + #intersections	Transport pheromone + mean road speed	Coordination of traffic lights based on transport pheromone

Table 3
Vehicle attributes in PGTS.

Vehicle type	#Vehicle for every 100 vehicles [36]	Maximum velocity (kmh)	Vehicle length (m)	Emission class
Petrol-based	75	150	4.7	PC_G_EU4
Diesel-based	4	150	4.7	PC_D_EU4
Truck	19	120	7.1	HDV
Bus	2	100	12.0	Bus

of acceleration, marking down GHG emissions considerably. Despite achieving competitive results in both CGVR and Rerouting -τ, the contribution of CGVR is more pronounced when the mean trip time is reduced to 976.9 s, as compared to 1008.8 s in Rerouting- τ.

Compared to Combination-τ, PGTS reduces CO_2 emission and fuel consumption by 37.7% and 37.6% respectively, promoting green transportation. Specifically, combination-τ aims to reduce congestion by solely adopting pheromone intensity in TLC-CDT and Rerouting-τ, while PGTS targets to reduce the transport emission by dispersing both upstream and downstream traffic. The integration of CTCL to disseminate the traffic on the congested roads into the corresponding downstream paths, and CGVR to probabilistically distribute vehicles away from the congested road to reduce upstream congestion, further justify its effectiveness in reducing transport emissions. The contribution of PGTS is

Fig. 5. Singapore Cityhall Map.

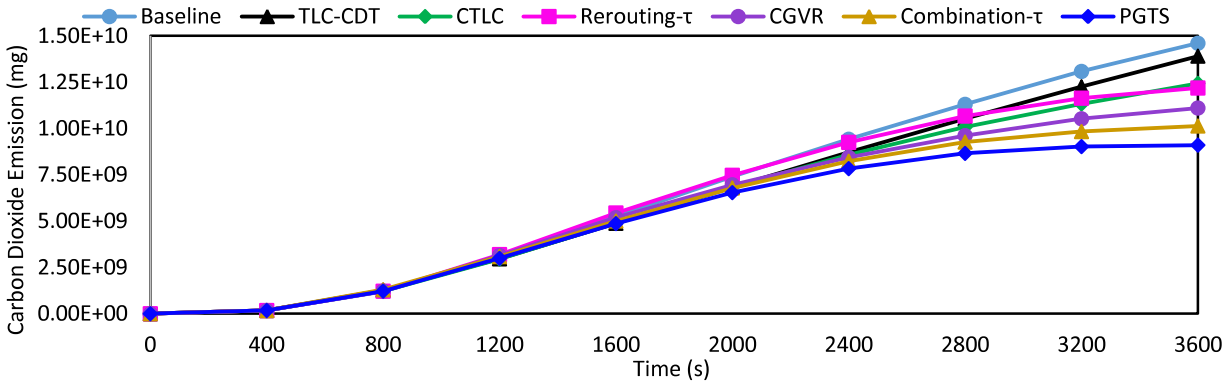

Fig. 6. Carbon dioxide emissions for all traffic management approaches.

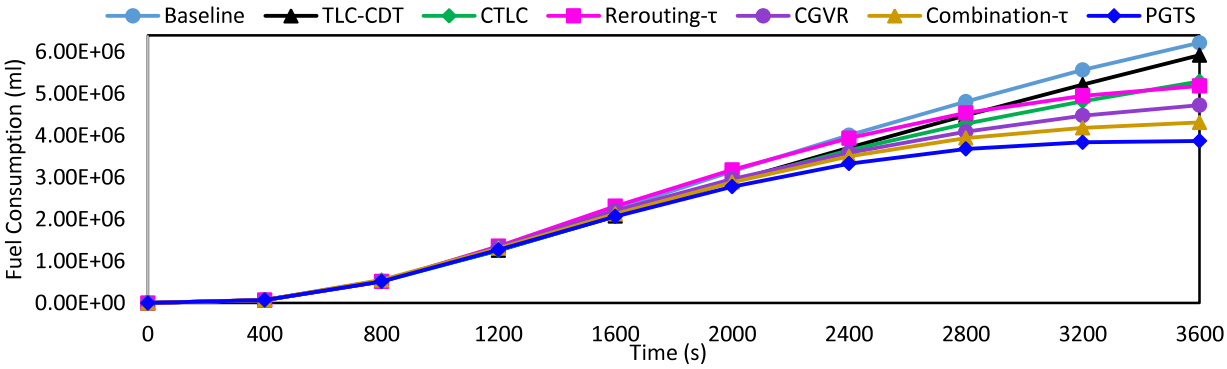

Fig. 7. Fuel consumption for all traffic management approaches.

even more significant when it enjoys a reduction in the number of congested roads beginning from 1600 s, indicating its ability to efficiently reduce urban congestion as compared to Combination-τ.

To further assess the effectiveness of PGTS, number of arrived vehicles and mean waiting time are investigated as shown in Table 4. Due to the non-normal distribution nature of the results, the Bias Corrected accelerated bootstrap confidence interval (BC_a) [39] is adopted to provide 95% Confidence Interval (CI) for samples considering the bias and skew. Among all approaches, the proposed PGTS yields the lowest mean waiting time and average trip time, justifying its potential to cut down the opportunity costs of congestion [40]. This is indeed consistent with the corresponding number of arrived vehicles, which is boosted to 3981 as compared to the baseline. Additionally, the environmental cost, specifically the fuel cost [40] is also marked down in PGTS, by virtue of the significantly lower GHG emissions and fuel consumption as compared to baseline.

4.3. Robustness test

To promote practicality, the proposed PGTS is evaluated under several uncertainties against variations of inherent routing and traffic light control parameter. Three key parameters are employed to assess the robustness of PGTS, specifically compliance rate, penetration rate, and traffic data rate. Compliance rate, C_r represents the percentage of drivers adhering to PGTS, whereas penetration rate, P_r refers to the percentage of drivers willing to

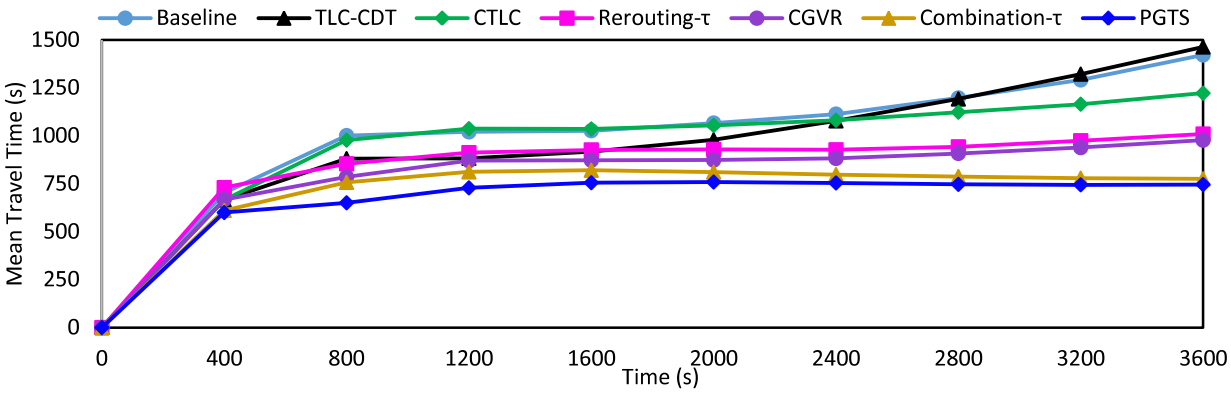

Fig. 8. Mean travel time for all traffic management approaches.

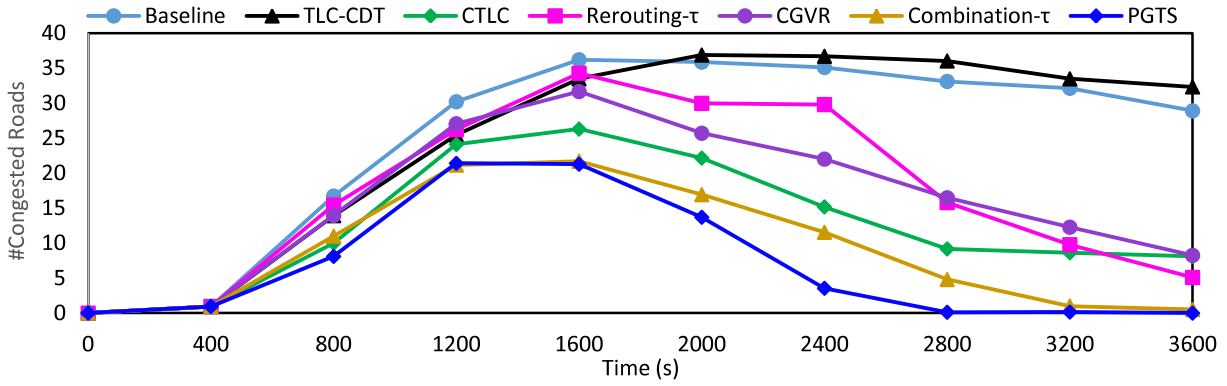

Fig. 9. Number of congested roads for all traffic management approaches.

Table 4
Summary of evaluation metrics of all traffic management approaches.

Approaches	Mean waiting time (e+06 s)		#Arrived vehicle		Trip time (s)	
	Mean	BC_a (95%CI)	Mean	BC_a (95%CI)	Mean	BC_a (95%CI)
Baseline	4.26	[4.20,4.31]	2448	[2404,2500]	1421.20	[1405.00,1433.00]
TLC-CDT	4.23	[4.16,4.32]	1987	[1933,2033]	1462.90	[1440.00,1490.00]
CTLC	3.18	[3.13,3.23]	2813	[2778,2850]	1221.80	[1209.00,1236.00]
Rerouting-τ	2.73	[2.69,2.77]	3648	[3626,3665]	1008.80	[997.00,1021.00]
CGVR	2.85	[2.77,2.92]	3554	[3514,3592]	976.89	[958.10,993.20]
Combination-τ	1.85	[1.82,1.88]	3866	[3840,3889]	775.45	[765.60,785.50]
PGTS	**1.82**	**[1.79,1.84]**	**3981**	**[3977,3985]**	**745.83**	**[738.90,752.60]**

Approaches	CO_2 emission (e+09 mg)		Fuel consumption (e+06 ml)	
	Mean	BC_a (95%CI)	Mean	BC_a (95%CI)
Baseline	14.60	[14.52,14.68]	6.22	[6.19,6.25]
TLC-CDT	13.91	[13.77,14.09]	5.92	[5.86,6.00]
CTLC	12.44	[12.36,12.54]	5.30	[5.26,5.34]
Rerouting-τ	12.19	[12.07,12.31]	5.19	[5.14,5.24]
CGVR	11.11	[10.97,11.24]	4.73	[4.67,4.79]
Combination-τ	10.14	[10.05,10.24]	4.32	[4.28,4.36]
PGTS	**9.10**	**[9.05,9.16]**	**3.88**	**[3.85,3.90]**

share their route intentions to PGTS. Traffic data rate T_r indicates the percentage of traffic light information that has successfully been conveyed among IAs to perform PCP and CTCL. In the event of missing traffic light information, the no-traffic-light scenario is employed to compute future pheromone.

Generally, there is an increase in fuel consumption, carbon dioxide emission, and mean travel time when the percentage of vehicle adhering PGTS is reduced. At the first glance, it is depicted that the line P_r lies above C_r. P_r is the percentage of drivers who share OD pairs, vehicles speed, and position, and also follow route guidance provided by IA. Hence, P_r affects the estimation of future pheromone in Eq. (3) and predicted transport pheromone in Eq. (7), as well as the performance of CGVR. On the contrary, C_r is the percentage of drivers who adhere to the route guidance, which affects only the efficiency of CGVR, justifying its better performance as compared to P_r. While achieving competitive performance with P_r and C_r at higher percentages, the difference in performance of T_r is more pronounced at lower percentages. T_r affects both forecasted transport pheromone in Eq. (7) and the efficiency of CTCL. Unlike P_r and C_r which have full coordination in CTCL, only a few traffic lights are coordinated at a lower percentage of T_r, leading to its lower performance at lower percentages.

In Figs. 10–12, the decrease of carbon dioxide emission, fuel consumption and mean trip time remains stable from $C_r = 0.4$ and $P_r = T_r = 0.6$. To further gauge the robustness of PGTS, the

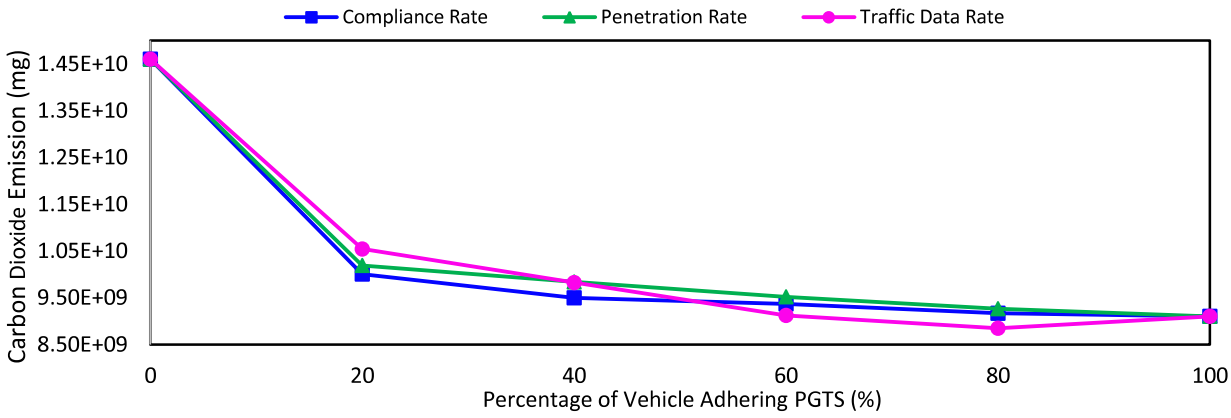

Fig. 10. Carbon dioxide emission of PGTS for different compliance rate, penetration rate and traffic data rate.

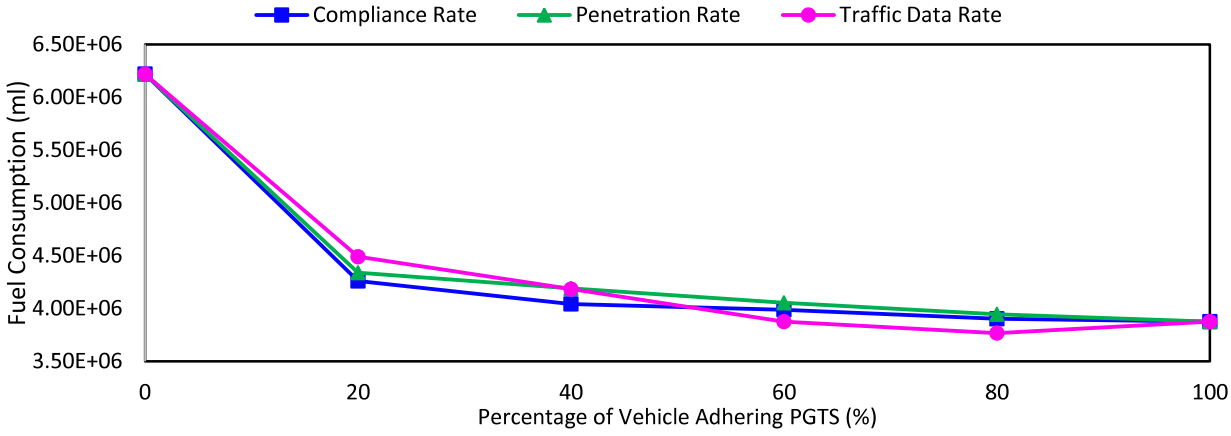

Fig. 11. Fuel consumption of PGTS for different compliance rate, penetration rate and traffic data rate.

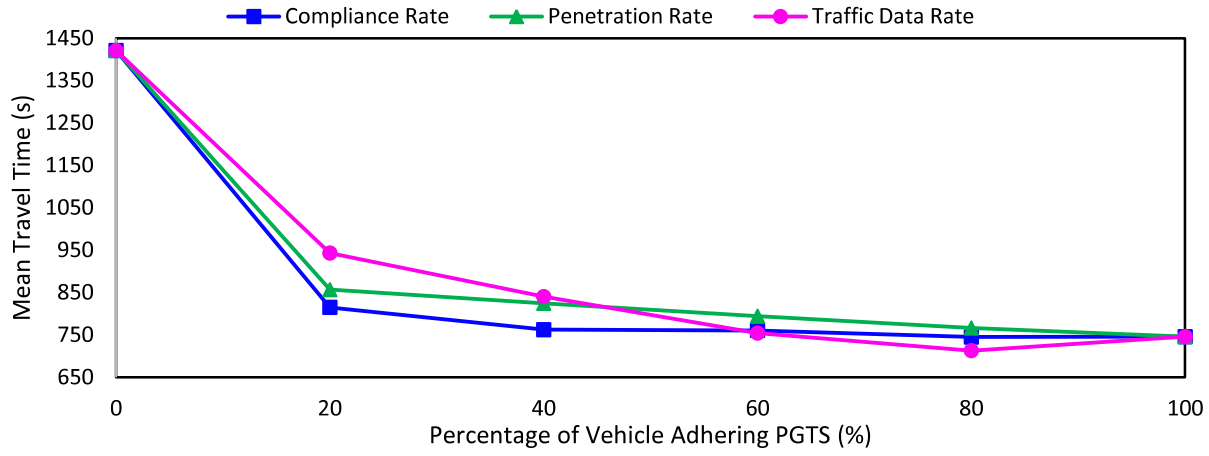

Fig. 12. Mean travel time of PGTS for different compliance rate, penetration rate and traffic data rate.

corresponding mean waiting time and number of arrived vehicles are summarized in Tables 5–7 for each key parameter. Considering the mean waiting time, competitive results are reported from $C_r = 0.2$, $P_r = T_r = 0.6$. Furthermore, the number of arrived vehicles is reported to remain relatively constant from $C_r = T_r = 0.4$, and $P_r = 0.6$. In summary, PGTS is robust against the compliance rate of [0.4,1.0], penetration rate of [0.6,1.0] and traffic data rate of [0.6,1.0], attesting that PGTS is effective and versatile even in the event of missing traffic light data and at a lower percentage of drivers adhering to PGTS.

4.4. Complexity analysis

Big O Notation has been adopted to access the time complexity of all approaches [41]. To ease explanation, a summary of the abbreviations of symbol is provided in Table 8, followed by the comparisons of computational costs across all approaches is illustrated in Table 9.

As all techniques adopt εSVR in traffic congestion forecasting, the computational costs are evaluated based on vehicle routing and traffic light control algorithms. The computational cost of TLC-CDT is $O[E_c+E_{nc}]$, as it adopts two different loops to find

Table 5
Summary of evaluation metrics of various compliance rates.

Compliance rate	#Arrived vehicle		Mean waiting time (e+06 s)		Average trip time (s)	
	Mean	BC_a (95%CI)	Mean	BC_a (95%CI)	Mean	BC_a (95%CI)
$C_r = 0$	2448	[2404,2500]	4.26	[4.20,4.31]	1421.20	[1405.00,1433.00]
$C_r = 0.2$	3790	[3778,3802]	1.97	[1.94,1.99]	815.11	[809.40,820.20]
$C_r = 0.4$	3907	[3890,3917]	1.82	[1.80,1.83]	762.33	[757.70,767.00]
$C_r = 0.6$	3946	[3935,3954]	1.84	[1.81,1.87]	760.73	[752.50,770.90]
$C_r = 0.8$	3967	[3960,3972]	**1.80**	**[1.78,1.83]**	**744.91**	**[737.90,751.00]**
$C_r = 1.0$	**3981**	**[3977,3985]**	1.82	[1.79,1.84]	745.83	[738.90,752.60]

Compliance rate	Fuel consumption (e+06 ml)		CO_2 emission (e+09 mg)	
	Mean	BC_a (95%CI)	Mean	BC_a (95%CI)
$C_r = 0$	6.22	[6.19,6.52]	14.60	[14.52,14.68]
$C_r = 0.2$	4.26	[4.24,4.28]	10.01	[9.96,10.05]
$C_r = 0.4$	4.04	[4.02,4.06]	9.50	[9.45,9.54]
$C_r = 0.6$	3.99	[3.96,4.03]	9.37	[9.31,9.46]
$C_r = 0.8$	3.90	[3.88,3.92]	9.17	[9.11,9.22]
$C_r = 1.0$	**3.88**	**[3.85,3.90]**	**9.10**	**[9.05,9.16]**

Table 6
Summary of evaluation metrics of various penetration rates.

Penetration rate	#Arrived vehicle		Mean waiting time (e+06 s)		Average trip time (s)	
	Mean	BC_a (95%CI)	Mean	BC_a (95%CI)	Mean	BC_a (95%CI)
$P_r = 0$	2448	[2404,2500]	4.26	[4.20,4.31]	1421.20	[1405.00,1433.00]
$P_r = 0.2$	3886	[3874,3898]	2.12	[2.10,2.15]	856.78	[849.70,864.40]
$P_r = 0.4$	3948	[3930,3955]	2.03	[2.00,2.06]	824.43	[816.90,833.20]
$P_r = 0.6$	3969	[3963,3973]	1.94	[1.91,1.97]	794.22	[785.40,802.80]
$P_r = 0.8$	**3981**	**[3976,3984]**	1.87	[1.84,1.90]	766.34	[759.90,774.60]
$P_r = 1.0$	3981	[3977,3985]	**1.82**	**[1.79,1.84]**	**745.83**	**[738.90,752.60]**

Penetration rate	Fuel consumption (e+06 ml)		CO_2Emission (e+09 mg)	
	Mean	BC_a (95%CI)	Mean	BC_a (95%CI)
$P_r = 0$	6.22	[6.19,6.52]	14.60	[14.52,14.68]
$P_r = 0.2$	4.34	[4.31,4.37]	10.19	[10.13,10.26]
$P_r = 0.4$	4.19	[4.16,4.22]	9.84	[9.78,9.92]
$P_r = 0.6$	4.05	[4.02,4.08]	9.52	[9.45,9.59]
$P_r = 0.8$	3.95	[3.92,3.97]	9.27	[9.22,9.33]
$P_r = 1.0$	**3.88**	**[3.85,3.90]**	**9.10**	**[9.05,9.16]**

Table 7
Summary of evaluation metrics of various traffic data rates.

Penetration rate	#Arrived vehicle		Mean waiting time (e+06 s)		Average trip time (s)	
	Mean	BC_a (95%CI)	Mean	BC_a (95%CI)	Mean	BC_a (95%CI)
$T_r = 0$	2448	[2404,2500]	4.26	[4.20,4.31]	1421.20	[1405.00,1433.00]
$T_r = 0.2$	3523	[3475,3572]	2.68	[2.62,2.76]	943.30	[924.30,962.20]
$T_r = 0.4$	3917	[3881,3937]	2.23	[2.17,2.32]	840.36	[823.10,863.20]
$T_r = 0.6$	3980	[3956,3990]	1.87	[1.83,1.96]	754.41	[742.50778.70]
$T_r = 0.8$	**3991**	**[3988,3993]**	**1.70**	**[1.67,1.73]**	**712.95**	**[706.00,720.90]**
$T_r = 1.0$	3981	[3977,3985]	1.82	[1.79,1.84]	745.83	[738.90,752.60]

Penetration rate	Fuel consumption (e+06 ml)		CO_2 Emission (e+09 mg)	
	Mean	BC_a (95%CI)	Mean	BC_a (95%CI)
$T_r = 0$	6.22	[6.19,6.52]	14.60	[14.52,14.68]
$T_r = 0.2$	4.49	[4.43,4.55]	10.54	[10.42,10.69]
$T_r = 0.4$	4.18	[4.12,4.27]	9.83	[9.69,10.02]
$T_r = 0.6$	3.88	[3.84,3.98]	9.12	[9.02,9.35]
$T_r = 0.8$	**3.77**	**[3.74,3.79]**	**8.85**	**[8.79,8.91]**
$T_r = 1.0$	3.88	[3.85,3.90]	9.10	[9.05,9.16]

the competing and non-competing relationships of a road segment. The time complexity of CTCL is quadratic owing to the application of nested loops in Algorithm 1 on page 10. Initially, the outer loop searches and coordinates all the congested roads (E_{con}). Within the first loop, the maximum transport pheromone intensity among all congested roads is obtained (E_{con}), followed by two different inner loops to coordinate upstream (E_{up}) and downstream (E_{down}) traffic of each congested road. It is also noticeable that the computational cost of Algorithm 2 is O [1]. While achieving a slight increase in computation cost, CTCL promotes the added value of generating green wave scenario through the coordination of traffic lights to mark down transport emissions as compared to TLC-CDT.

In Rerouting-τ, the first term finds the number of congested roads (E_{con}), while the second term employs a nested loop that reroutes vehicles based on pheromone intensity. Particularly, the outermost loop searches all congested roads (E_{con}). Within the first loop, it finds the maximum pheromone intensity in all congested roads (E_{con}). The second loop iteratively searches all neighboring roads (E_{nei}) and finds the vehicles (V) having intentions to traverse the congested road. The innermost loop distributes vehicles V by using kSP, with the combined computational cost

Table 8
A abbreviations of symbols adopted in Big O Notation in Table 9.

Symbol	Name
E_c	Number of competing roads
E_{nc}	Number of non-competing roads
E_{con}	Number of congested roads
E_{up}	Number of upstream roads
E_{down}	Number of downstream roads
E_{nei}	Number of neighboring roads
E_{path}	Number of roads in a digraph
V	Number of intentional vehicles
G_{od}	Number of *OD* pairs within a road segment
d	Number of available d paths in dkSP (Eq. 9)
k	Number of available k paths in kSP

Table 9
Big O Notation for all approaches.

Approaches	Big O Notation
TLC-CDT	$O[E_c+E_{nc}]$
CTLC	$O[E_{con}(E_{con}+ E_{up} + E_{down})]$
Rerouting-τ	$O[E_{con}+E_{con}(E_{con}+ E_{nei} (V+ kV^2(E_{path}+ V\log V)))]$
CGVR	$O[E_{con}+E_{con}(E_{con}+ E_{nei} (V + G_{od}(dV^2(E_{path} +V\log V)))]$
Combination-τ	$O[E_{con}(E_{con}+ E_{nei} (V+ kV^2(E_{path}+ V\log V)))]$
PGTS	$O[E_{con}(E_{con}+ E_{nei} (V + G_{od}(dV^2(E_{path} +V\log V))))]$

of $kV^2(E_{path}+ V\log V)$. The main difference between CGVR and Rerouting-τ is the additional loop in searching each OD pair (G_{od}). Compared to the conventional *kSP*, the application of dkSP in CGVR reduces the computational effort in each OD pair as $d \leq k$ as per Eq. (9) for $\delta \leq T_{con} \leq 1$. Overall, the contribution of CGVR in mitigating congestion and reducing transport emission outweigh the relatively marginal increase in computational effort as compared to Rerouting-τ.

The computational cost of PGTS is the sum of CGVR and CTLC whereas the computational effort of Combination-τ is the sum of Rerouting-τ and TLC-CDT. It is worth noticing that the computational costs of the nest loop in the vehicle routing algorithms dominate in both PGTS and Combination-τ. Therefore, the computational cost of PGTS is approximated to be $O[E_{con}(E_{con}+ E_{nei} (V + G_{od}(dV^2(E_{path} +V\log V)))]$ while the computational effort of Combination-τ is estimated to be $O[E_{con}(E_{con}+ E_{nei} (V+ kV^2(E_{path}+ V\log V)))]$. While achieving competitive time complexity with TLC-CDT, PGTS shows a substantial improvement in performances compared to Combination-τ. Additionally, each IA in PGTS is only responsible for managing the transport pheromone of four road links in a bidirectional four-way intersection. The localized communication among IAs further justifies the efficiency of PGTS.

4.5. Statistical test

In addition to robustness tests, two statistical tests are performed using the obtained results from forty experiments to further gauge the performance of PGTS. As the focus is centered on reducing GHG emissions and urban congestion, these statistical tests are conducted to assess the performance in terms of carbon dioxide emissions, fuel consumption, mean travel time and number of congested roads. By following the guidance in [42], Friedman's non-parametric test is conducted to check if there are significant differences among all traffic management approaches. Considering the 99% confidence interval in a χ^2 distribution with 6° degree of freedom, the largest p-value from these important performance indices is lower than α-value of 0.01. It can then be concluded that there exists significant differences among all approaches, being PGTS the one with the lowest rank as depicted in Table 10.

To evaluate the statistical significance of the better performance of PGTS, Holm's post hoc test is then carried out by taking PGTS as the control approach. In Table 11, it is shown that all p-values are lower than the adjusted α-values in all performance metrics, affirming that PGTS is significantly better than all other approaches at a 95% confidence level.

5. Conclusion

In this paper, a Pheromone-based Green Transportation System (PGTS) is proposed to reduce transport emissions with threefold contributions. First, PGTS is a proactive system that employs an online epsilon-Support Vector Regression model to forecast traffic congestion. Second, the traffic on the predicted congested roads is diverged to the corresponding downstream paths through a Coordinated Traffic Light Control (CTLC) to generate green wave scenario. Third, a Cooperative Green Vehicle Routing (CGVR) takes a further step to probabilistically reroute upstream vehicles from entering the congested roads, dispersing the upstream traffic to prevent worsening of traffic congestion.

Compared to TLC-CDT which diverges congestion based on competing relationships with neighbors, CTCL which coordinates the downstream traffic lights enables vehicles to traverse multiple intersections, effectively reducing transport emissions. While Rerouting-τ distributes vehicles based on pheromone intensity, CGVR reduces fuel consumption by adopting an additional mean road speed parameter to select greener paths for vehicles. As Combination-τ reduces congestion by fusing TLC-CDT and Rerouting-τ, PGTS promotes the added values by disseminating upstream and downstream traffic through CGVR and CTCL respectively. This integration allows vehicles traversing multiple intersections with fewer frequencies of acceleration, efficiently marking down fuel consumption. Using Singapore traffic data, PGTS outperforms other existing approaches in reducing carbon dioxide emissions by 37.7%, fuel consumption by 37.6%, mean travel time by 47.5%, mean waiting time by 57.3%, and increasing number of arrived vehicles by 62.6%. The contribution of PGTS is even more pronounced, when promising results are obtained at a lower compliance rate of 40%, penetration rate of 40% and traffic data rate of 60%. In future, PGTS can be extended to investigate the impacts of unforeseen events such as accidents and adverse weather conditions.

Acknowledgments

The authors would like to thank Monash University Malaysia for the research support. In addition, the authors sincerely appreciate and thank anonymous reviewers and editorial board for providing constructive comments to enhance the quality of the paper.

Table 10
Average rankings returned by Friedman's test.

Approaches	Carbon dioxide	Fuel consumption	Mean travel time	#Congested roads
Baseline	6.91	6.91	6.38	6.31
TLC-CDT	6.06	6.06	6.62	6.69
CTLC	4.74	4.75	5.00	4.30
Rerouting-τ	4.26	4.25	3.62	3.30
CGVR	3.00	3.00	3.38	4.36
Combination-τ	2.02	2.02	1.78	1.68
PGTS	**1.00**	**1.00**	**1.22**	**1.36**

Table 11
Results returned from Holm's post-hoc tests with PGTS used as the control approach.

Approaches	Carbon dioxide		Fuel consumption		Mean travel time		#Congested roads	
	P-values	Adjusted α-values	*P*-values	Adjusted α-values	*P*-values	Adjusted α-values	*P*-values	Adjusted α-values
Baseline	3.56e−08	8.33e−03	3.55e−08	1.67e−02	3.57e−08	8.33e−03	3.45e−08	3.33e−02
PVR	3.56e−08	8.33e−03	3.56e−08	4.17e−02	3.57e−08	8.33e−03	3.46e−08	4.17e−02
FCPVR	3.57e−08	4.17e−02	3.54e−08	8.33e−03	3.57e−08	8.33e−03	3.38e−08	2.50e−02
TTPVR	3.56e−08	8.33e−03	3.55e−08	1.67e−02	3.57e−08	8.33e−03	2.98e−08	8.33e−03
MSPVR	3.57e−08	4.17e−02	3.55e−08	1.67e−02	3.57e−08	8.33e−03	3.26e−08	1.67e−02
CDPVR	3.56e−08	8.33e−02	3.56e−08	4.17e−02	2.07e−04	5.00e−02	1.77e−03	5.00e−02

Declaration of competing interest

No author associated with this paper has disclosed any potential or pertinent conflicts which may be perceived to have impending conflict with this work. For full disclosure statements refer to https://doi.org/10.1016/j.asoc.2019.105486.

References

[1] M.R. Jabbarpour, A. Jalooli, E. Shaghaghi, R.M. Noor, L. Rothkrantz, R.H. Khokhar, N.B. Anuar, Ant-based vehicle congestion avoidance system using vehicular networks, Eng. Appl. Artif. Intell. 36 (2014) 303–319.

[2] J.S. Pan, M.A. Khan, I.S. Popa, K. Zeitouni, C. Borcea, Proactive vehicle re-routing strategies for congestion avoidance, in: 2012 8th IEEE International Conference on Distributed Computing in Sensor Systems, 2012, pp. 265–272.

[3] J.S. Pan, I.S. Popa, C. Borcea, Divert: A distributed vehicular traffic re-routing system for congestion avoidance, IEEE Trans. Mob. Comput. 16 (2017) 58–72.

[4] A. Jovanović, M. Nikolić, D. Teodorović, Area-wide urban traffic control: A bee colony optimization approach, Transp. Res. C 77 (2017) 329–350.

[5] X. Li, J.-Q. Sun, Signal multiobjective optimization for urban traffic network, IEEE Trans. Intell. Transp. Syst. (2018) 1–9.

[6] D. Mckenney, T. White, Distributed and adaptive traffic signal control within a realistic traffic simulation, Eng. Appl. Artif. Intell. 26 (2013) 574–583.

[7] C. Lin, K.L. Choy, G.T. Ho, S.H. Chung, H. Lam, Survey of green vehicle routing problem: past and future trends, Expert Syst. Appl. 41 (2014) 1118–1138.

[8] M.R. Jabbarpour, R.M. Noor, R.H. Khokhar, Green vehicle traffic routing system using ant-based algorithm, J. Netw. Comput. Appl. 58 (2015) 294–308.

[9] G. Poonthalir, R. Nadarajan, A fuel efficient green vehicle routing problem with varying speed constraint (F-GVRP), Expert Syst. Appl. 100 (2018) 131–144.

[10] Y. Xiao, A. Konak, The heterogeneous green vehicle routing and scheduling problem with time-varying traffic congestion, Transp. Res. E 88 (2016) 146–166.

[11] Y. Niu, Z. Yang, P. Chen, J. Xiao, Optimizing the green open vehicle routing problem with time windows by minimizing comprehensive routing cost, J. Clean Prod. 171 (2018) 962–971.

[12] A.C. Olivera, J. García-Nieto, E. Alba, Reducing vehicle emissions and fuel consumption in the city by using particle swarm optimization, Appl. Intell. 42 (2015) 389–405.

[13] L. D'Acierno, M. Gallo, B. Montella, An ant colony optimisation algorithm for solving the asymmetric traffic assignment problem, European J. Oper. Res. 217 (2012) 459–469.

[14] J. He, Z. Hou, Ant colony algorithm for traffic signal timing optimization, Adv. Eng. Softw. 43 (2012) 14–18.

[15] Z. Cao, S. Jiang, J. Zhang, H. Guo, A unified framework for vehicle rerouting and traffic light control to reduce traffic congestion, IEEE Trans. Intell. Transp. Syst. 18 (2017) 1958–1973.

[16] D. Krajzewicz, M. Behrisch, P. Wagner, R. Luz, M. Krumnow, Second generation of pollutant emission models for SUMO, in: Modeling Mobility with Open Data, Springer, 2015, pp. 203–221.

[17] S. Jiang, J. Zhang, Y.-S. Ong, A pheromone-based traffic management model for vehicle re-routing and traffic light control, in: Proceedings of the 2014 International Conference on Autonomous Agents and Multi-Agent Systems, 2014, pp. 1479–1480.

[18] C. Miao, H. Liu, G.G. Zhu, H. Chen, Connectivity-based optimization of vehicle route and speed for improved fuel economy, Transp. Res. C 91 (2018) 353–368.

[19] D.H. Stolfi, E. Alba, Green swarm: Greener routes with bio-inspired techniques, Appl. Soft. Comput. 71 (2018) 952–963.

[20] K.L. Soon, J.M.-Y. Lim, R. Parthiban, M.C. Ho, Proactive eco-friendly pheromone-based green vehicle routing for multi-agent systems, Expert Syst. Appl. 121 (2019) 324–337.

[21] S. Wang, S. Djahel, Z. Zhang, J. McManis, Next road rerouting: A multiagent system for mitigating unexpected urban traffic congestion, IEEE Trans. Intell. Transp. Syst. 17 (2016) 2888–2899.

[22] L.-W. Chen, C.-C. Chang, Cooperative traffic control with green wave coordination for multiple intersections based on the internet of vehicles, IEEE Trans. Syst. Man, Cybern. Syst. 47 (2017) 1321–1335.

[23] R. Blokpoel, W. Niebel, Advantage of cooperative traffic light control algorithms, IET Intell. Transp. Syst. 11 (2017) 379–386.

[24] J. Jin, X. Ma, Hierarchical multi-agent control of traffic lights based on collective learning, Eng. Appl. Artif. Intell. 68 (2018) 236–248.

[25] A.G. Sims, K.W. Dobinson, The sydney coordinated adaptive traffic (SCAT) system philosophy and benefits, IEEE Trans. Veh. Technol. 29 (1980) 130–137.

[26] J.H. Kell, I.J. Fullerton, M.K. Mills, Traffic Detector Handbook, 1990, Retrieved from: http://www.fhwa.dot.gov/publications/research/safety/ip90002/ip90002pdf.

[27] S. Kurihara, H. Tamaki, M. Numao, J. Yano, K. Kagawa, T. Morita, Traffic congestion forecasting based on pheromone communication model for intelligent transport systems, in: IEEE Congress on Evolutionary Computation, 2009, pp. 2879–2884.

[28] K.L. Soon, J.M.-Y. Lim, R. Parthiban, Extended pheromone-based short-term traffic forecasting models for vehicular systems, Eng. Appl. Artif. Intell. 82 (2019) 60–75.

[29] C.-C. Chang, C.-J. Lin, LIBSVM: a library for support vector machines, ACM Trans. Intell. Syst. Technol. 2 (2011) 27.

[30] A. Ermagun, D. Levinson, Spatiotemporal traffic forecasting: review and proposed directions, Transp. Rev. (2018) 1–29.

[31] Z. Ma, G. Luo, D. Huang, Short term traffic flow prediction based on online sequential extreme learning machine, in: 2016 Eighth International Conference on Advanced Computational Intelligence, ICACI, 2016, pp. 143–149.

[32] O. Jun, L. Jun, C. Min, Parameter estimation of Logit route choice model with unified parameter, in; Second International Conference on Intelligent Computation Technology and Automation, ICICTA. vol. 2, 2009, pp. 148–151.

[33] X. Zhao, C. Wan, H. Sun, D. Xie, Z. Gao, Dynamic rerouting behavior and its impact on dynamic traffic patterns, IEEE Trans. Intell. Transp. Syst. 18 (2017) 2763–2779.

[34] J. Li, Q. Wu, D. Zhu, Route guidance mechanism with centralized information control in large-scale crowd, in: 2009 International Joint Conference on Artificial Intelligence, 2009, pp. 7–11.

[35] M. Behrisch, L. Bieker, J. Erdmann, D. Krajzewicz, Sumo–simulation of urban mobility, in: The Third International Conference on Advances in System Simulation, SIMUL 2011, vol. 42, 2011, Barcelona, Spain.

[36] Land transport authority Singapore, datamall, 2018, Retrieved from: https://www.mytransport.sg/content/mytransport/home/dataMall.html.

[37] A. Wegener, M. Piórkowski, M. Raya, H. Hellbrück, S. Fischer, J.-P. Hubaux, TraCI: an interface for coupling road traffic and network simulators, in: Proceedings of the 11th Communications and Networking Simulation Symposium, 2008, pp. 155–163.

[38] J.C. Dias, P. Machado, D.C. Silva, P.H. Abreu, An inverted ant colony optimization approach to traffic, Eng. Appl. Artif. Intell. 36 (2014) 122–133.

[39] B. Efron, Better bootstrap confidence intervals, J. Amer. Statist. Assoc. 82 (1987) 171–185.

[40] S. Jayasooriya, Y. Bandara, Measuring the Economic costs of traffic congestion, in: Engineering Research Conference, MERCon, 2017, pp. 141–146.

[41] I. Chivers, J. Sleightholme, An introduction to algorithms and the big o notation, in: Introduction to Programming with Fortran, Springer, 2015, pp. 359–364.

[42] J. Derrac, S. García, D. Molina, F. Herrera, A practical tutorial on the use of nonparametric statistical tests as a methodology for comparing evolutionary and swarm intelligence algorithms, Swarm Evol. Comput. 1 (2011) 3–18.